

EFFECT OF SILANE SIZING ON POLYMER-GLASS ADHESION

H. Dvir and M. Gottlieb

Chemical Engineering Department and IKI Institute for Nanoscale Science and Technology, Ben Gurion University, Beer Sheva 84105, Israel
mosheg@cs.bgu.ac.il

SUMMARY

Several types of common polymers were deposited on glass slides sililated with organofunctional silanes. The extent of surface coverage, adsorbed layer thickness and topology were experimentally determined. The strength of polymer interaction with the silane treated glass was investigated using contact-mode AFM. The interaction strength to the surface was found to be dominated by hydrophobic/hydrophilic interactions and hydrogen bonds.

Keywords: Interface, polymer, Silane surface treatment, Adhesion, Glass-reinforced composite, AFM, Contact-mode

INTRODUCTION

The properties of polymer-based composites depend to a large degree, on the interfacial interaction between the polymeric matrix and the additives. Superior mechanical properties, which comprise the basic requirement for most composite formulations, are commonly achieved using fibers. In an ideal composite, a well-established interface between the fiber and the polymer matrix will disperse the external load to the rigid fiber, which, in turn, will enhance the mechanical strength of the material. In general, the adhesion between polymeric materials and additives or fillers is weak due to poor compatibility, wettability, and bonding. Coupling agents, usually introduced as fiber sizing, are commonly used in order to overcome the chemical incompatibility between the two components, thereby improving their mutual affinity. Increased affinity is manifested by enhanced interfacial forces, varying in strength from strong covalent bonds to weak van der Waals (VDW) interactions. In the case of commercial glass fibers, organo-silane-based coupling agents are most commonly used. The general chemical structure of organofunctional silane coupling agents is $(RO)_3SiX$, where RO is an alkoxy group and X is the organofunctional group [1,2]. There is a large variety of possible organofunctional groups and the specific group for a given composite is selected based on its affinity to the polymer matrix. The alkoxy groups hydrolyze in aqueous solution to form hydroxyl groups, which react with the silanol groups on the fiber surface through a condensation reaction, subsequently forming a crosslinked silane layer by further reaction between adjacent silane molecules. Contradictory findings have been reported on how silane treatments affect the mechanical properties of composites. Both increase [3,4] and decrease [5] in elastic modulus have been observed while some researchers have even declared that silane treatments have no effect on mechanical properties [6,7]. Variations in the effect silane treatments have on composite

mechanical properties may result from indirect consequences such as interaction of the sizing with other fillers, microcrazes, or accelerated microphase separation, and need not necessarily be the result of silane-polymer interfacial interactions. Unfortunately, the direct information necessary to understand the impact of silane treatments on the polymer-fiber interface is difficult to obtain under processing conditions of composite materials. Most available data on the interfacial adhesion strength have been obtained from macro-mechanical tests (e.g. tensile test) on complete formulate composites [1] or micro-mechanical tests (e.g. "pull-out" test, fragmentation test) on single particle composites [8]. Yet, these techniques cannot reveal the exact nature of the interfacial behavior. Our work evaluates the interaction strength between the polymer and the silane treated glass using the micromanipulation AFM "scratch resistance" technique described in detail elsewhere [9].

EXPERIMENTAL

Materials

Four types of sililation agents (two polar two non polar, two reactive, two inert) were used: (3-aminopropyl)trimethoxysilane (**APS**), (3-glycidyoxypropyl)trimethoxysilane (**GPS**), trimethoxy(propyl)silane (**TPS**), vinyltrimethoxysilane (**VS**). Sililation agents were obtained from Aldrich, USA and used without any further purification

Five types of polymers were tested:

Isotactic polypropylene (PP), $M_w=340K$, P.D.=3.5, ($M_e=6800$) [10];

Low density polyethylene (LDPE), $M_w=125K$, P.D.=3.88, ($M_e\approx 800$) [10];

Polystyrene (PS), $M_w=350K$, P.D.=2.05, ($M_e=17K$) [10];

Polypropylene-graft-maleic anhydride (PP-g-ma), $M_w=9100$, P.D.=2.33;

Polyethylene-graft-maleic anhydride (PE-g-ma).

The reported amount of grafted maleic anhydride in PP-g-ma and PE-g-ma was 1% - 5% w/w. The solvents used for polymer removal and rinsing of the glass slides were Xylene (HPLC grade, Aldrich, USA) and Toluene (analytical grade EIL, Israel).

Sample Preparation

The procedure for sample preparation is described in great detail elsewhere [9]. Only a summary highlighting the main steps is provided here. Standard 76x26mm microscope glass slides were first inserted into the sulfochromic cleaning solution and then rinsed in distilled water and in methanol in order to remove excess cleaning solution. Sililating solution was prepared by mixing methanol, distilled water, acetic acid, and the desired silane coupling agent. The silane layer was formed by submerging clean glass slides in the solution.

Polymer granules were placed on top of the glass slides and heated for ~120 minutes in an oven at temperatures well above T_m (T_g for PS). The slides were then removed from the oven and cooled to room temperature. The entire sample was subsequently placed in a bath filled with a good solvent for the polymer, (xylene or toluene) at a temperature near its boiling point. Each glass slide was rinsed at least three times with the hot, clean, good solvent for 5-10 min each time. We based our determination that three cycles of rinsing were sufficient to extract most of the non-adsorbed polymer chains on the observation that the thickness of the polymer layer, as measured by Optical Phase

Interference Microscopy (OPIM), did not decrease any further. We assume that only the most strongly adhered polymer chains will remain on the glass surface after this procedure. This assumption is valid for cases in which the adsorption kinetics is fast in comparison with the diffusion of polymer chains in the solution; thus, the adsorption is irreversible and the initial chains are retained and adsorbed onto the surface [9].

AFM Measurements

Measurements were performed using a Dimension 3100 SPM (Digital Instruments Veeco, Santa Barbara, CA 93117, USA). The cantilever (MikroMasch, NSC12, L = 250 μm) is made of doped single crystal silicon; the tip radius is typically 10 nm. The force constant of this cantilever was $0.43 \text{ N/m} \pm 0.1 \text{ N/m}$ determined according to the reference cantilever method against force calibrated cantilevers (CLFC-NOBO, Thermo-Microscopes Veeco) [9]. The AFM was used in two different modes:

- i) The topographies of various glass surfaces and the polymer layers deposited on them were evaluated by analysis of images obtained by tapping mode AFM. Images were constructed from 512 line scans over a 1×1 or $4 \times 4 \mu\text{m}^2$ squares at a scan rate of 1 Hz.
- ii) The interaction strength between an adsorbed polymer and the surface was evaluated by contact-mode AFM experiments. In these micromanipulation "scratch resistance" measurements, $0.5 \times 0.5 \mu\text{m}^2$ squares were scanned in contact-mode (512 lines, 4 Hz) with the set point voltage varied between 0.1 V and 2.4 V. During each scan, some or all of the polymer, depending on the set point, was removed by the AFM tip. The critical voltage (i.e. force) necessary to completely remove the polymer layer was determined from the experiment. Full details of these contact mode AFM measurements are discussed elsewhere [9].

Optical Phase Interference Microscopy (OPIM)

Surface topography was imaged with Optical Phase Interference Microscopy - OPIM, also known as Scanning White-Light Interference Microscopy. The instrument (New View 200, Zygo, Middlefield, CT 06455-0448, USA) produces 3-D images of the sample surface from which the polymer layer thickness could be determined from the height difference between the polymer surface and the exposed substrate. The procedure for determination of polymer film thickness is described in detail elsewhere [9].

RESULTS AND DISCUSSION

OPIM Analysis

The thicknesses of the polymer films remaining on the surface after rinsing with the boiling "good solvent" were measured using OPIM. The polymer layer was scratched all the way down to the glass substrate with a sharp, metallic object, but no damage to the glass substrate was detected [9,11]. In the case of grossly inhomogeneous film thickness, OPIM and AFM examinations were conducted only on the regions of the samples with the thinnest layers. Exclusion of thicker films was motivated by the desire to minimize effects of the polymer bulk in evaluation of polymer-surface interactions.

The three homopolymers (PP, LDPE and PS) and PE-g-ma were found to have characteristic film thicknesses irrespective of the type of surface treatment. The film

thickness for the maleic anhydride-graft-PP varied considerably with the type of surface treatment. The results for the film thickness H_{film} of the adsorbed homopolymers are presented in Table 1 along with characteristic molecular dimensions.

Table 1: Thicknesses of adsorbed polymer layers and polymer chain properties.

Polymer	H_{film} (nm)	M_w ($\times 10^3$)	DP ($\times 10^3$)	r_0^2/M [10] ($\times 10^{-3} \text{nm}^2$)	r_0 (nm)	N ($\times 10^3$)	n_{lp}
PP	17-18	340	8.1	6.94	49	1.8	65-70
PS	8-10	350	3.4	4.37	39	0.5	60-78
LDPE	40	125	4.5	14.0	42	0.7	15

Let us review the conformation of the chains on the surface. Initially, the polymer is in a melt state and the chain dimensions are $r_0 \sim aN^{0.5}$, where a is the size of the Kuhn step length and N is the number of repeat units [12, 13] which usually differs from the degree of polymerization (DP). While the polymer is rinsed with the boiling good solvent the chains expand to the Flory radius $r_F \sim aN^{0.59}$ [12, 13]. A fraction of the chains, those not in contact with the surface or only weakly adsorbed to it, will wash away. Upon removal of the solvent we expect only those chains that were in close contact with the surface and strongly adsorbed to it (i.e. many contact points) to remain. The chain segments between the anchoring points to the surface (chain loops and trains with N_x units per loop) will assume brush-like conformations with loop dimensions (approximately equal to film thickness) $H_{\text{film}} \sim aN_x^{0.83} < r_0$ [14]. Table 1 lists the dimensions of the polymer chains along with the film thickness. We observe that in all three cases the film thickness is indeed smaller than r_0 . From the available data we may estimate the number of loops per chain $n_{\text{lp}} \sim N/N_x$.

Although the results obtained for LDPE from the above analysis are also tabulated in Table 1, these results probably underestimate to a considerable extent the number of contacts because of the large degree of branching characteristic of this polymer sample.

Finally, the analysis above assumes that the chains are in their melt state. Although the experiments are carried out at temperatures above T_g for PP and LDPE but below T_m , we assume that a thin layer of polymer chains strongly adsorbed to the surface will not crystallize and the chains retain their melt-like conformations. The yet unresolved question of crystallization in adsorbed polymer layers has been addressed by others [15], we have not examined this issue here.

As previously pointed out [14, 16, 17, 18], the thickness of a polymer film in the absence of a solvent depends on the balance between chain entropy and the strength of interaction between the polymer and the surface. Results showing only minor variations in film thicknesses for the different surface treatments indicate that the interactions of these polymers with the surface treatments are not very different in nature. This observation will be further substantiated below.

In contrast with all the other polymers examined here, PP-g-ma films showed large variations in film thicknesses between the different surface treatments. The lowest

thickness values were recorded for the two hydrophobic alkylsilanes: 9nm on TPS and 10nm on VS. An intermediate value was measured on GPS (30nm) and the highest value, (50nm), was obtained for either APS or untreated glass. These values should be contrasted with the thicknesses of PP films (17-18 nm) and PE-g-ma (5-7 nm).

The average contour length of a PP-g-ma chain is approximately 40 times smaller than that of PP, yet the film thickness of PP-g-ma is considerably larger than that of PP on untreated glass and on two out of the four surface treatments. Although the amount of grafted maleic anhydride (ma) on the chain is relatively small (<5%), we have to conclude that surface behavior is completely dominated by specific interactions between the grafted ma and surface groups and possible intermolecular reactions between adjacent ma groups. The higher reactivity of the non-alkyl treatments and the role it plays in the formation of these thicker layers requires further examination.

AFM Imaging

Representative AFM images of the adsorbed polymer layers are depicted in Fig. 1 showing PP films on VS and APS as well as LDPE on VS. The roughness RMS and Peak to Valley (P-V) values for the three homopolymers are listed in Table 2.

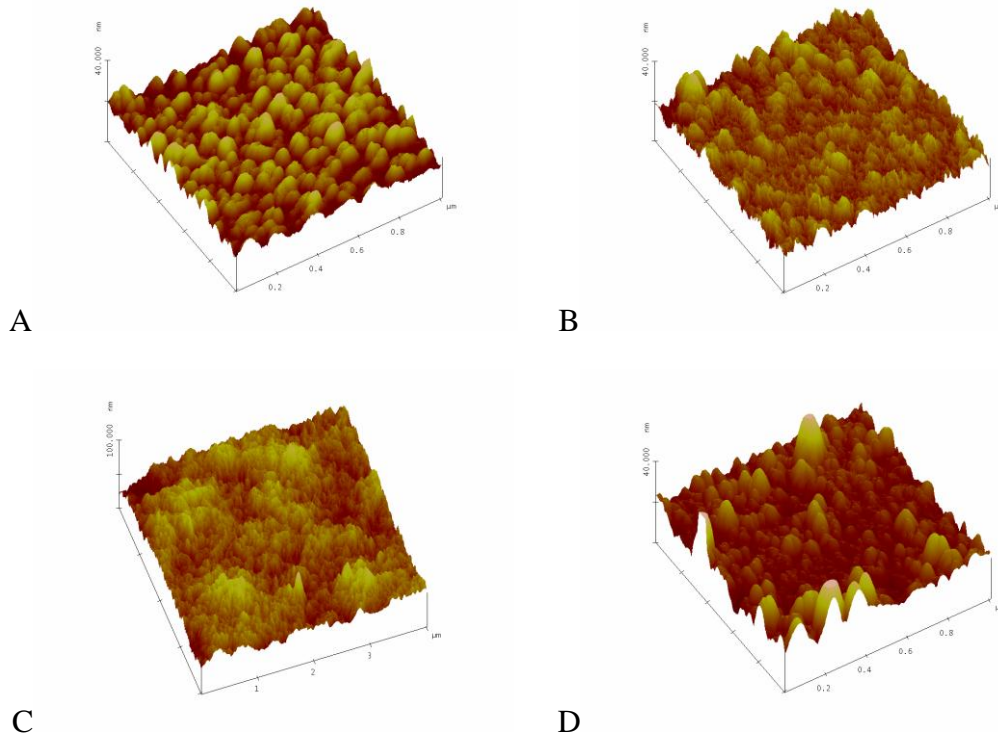


Fig. 1. AFM images of polymer layer on glass: A) PP deposited on VS, B) PP on APS, C) LDPE on VS, D) PP-g-ma on GPS

Two different topologies are identified for the surface of PP layers on glass: one characteristic of the two hydrophobic alkylsilane treatments (VS, TPS) and the other characteristic of the three hydrophilic surfaces: untreated glass, APS, and GPS. The

surface topologies of PP on TPS and VS are composed of densely packed smooth ellipsoidal protrusions relatively homogeneous in size and shape (cf. Fig. 1a). In contrast, the polymer layout on the hydrophilic surfaces is composed of jagged edged 'mountains' and 'craters' (cf. Fig. 1b). The same characteristic grouping is also manifested in the RMS values. In addition, while the two alkylsilane treatments maintain the typical 10:1 ratio of P-V to RMS, the ratio is considerably higher for the three other surfaces, indicating once again the more rugged features of these surfaces. It is possible to conclude from the comparison of the two topologies that the affinity (or wetting) of the hydrophobic PP to alkylsilane treated surfaces is higher than its affinity to the three other surfaces. We were unable to detect clear trends in the surface characteristics and behavior of either LDPE or PS. There are also no discernible trends in the RMS and P-V values for PS. However, as in the case of PP, the RMS values for the LDPE are higher for the hydrophobic treatments (VS, TPS) than those of the hydrophilic surfaces. The roughness RMS for LDPE on an APS treated surface is an exception to this trend.

The surfaces of PP-g-ma films are characterized in all cases by smooth, curved, protrusions of irregular height and separation as seen in Fig. 1d. The difference between the various silane treatments is manifested in the P-V values: 55nm for untreated glass, APS, and GPS, and 35nm for VS and TPS. These results are in agreement with the film thickness determined by OPIM: thicker film (30-50 nm) on the hydrophilic surfaces and thinner film (9-10 nm) on the two hydrophobic treatments.

Table 2: Roughness RMS and Peak to Valley (P-V) of polymer layers adsorbed to the different glass surfaces as measured by AFM imaging (all values are in nm)

polymer	PP		PE		PS	
	RMS	P-V	RMS	P-V	RMS	P-V
Untreated	1.6	53	3.6	36	6.4	41
APS	2.9	47	6.5	45	0.9	10
GPS	2.5	44	3.8	38	5.5	39
VS	4.3	43	6.5	53	1.2	18
TPS	4.5	42	7.1	57	1.2	15

Contact Mode AFM Measurements

AFM measurements were employed to assess the polymer-surface adhesion strength. The measurement's main feature is its use of contact-mode AFM as a tool to scratch off the polymer layer adsorbed on the solid surface. Fig. 2 depicts tapping mode AFM images of PE deposited on untreated glass prior and subsequent to the application of the contact-mode scan used to carve out the recess in the polymer layer and clearly illustrates the technique.

The results of the AFM adhesion strength experiments are summarized in Table 3. The measured adhesion forces range from 7 nN to 134 nN and for most cases they lie in the range of 30-70 nN. These values are intermediate to the values measured for typical attraction VDW forces and those required to break covalent bonds ($>1 \mu\text{N}$ [19]). Since our analysis indicates that the polymers adhere to the surface via large number of anchoring points, we conclude that the adhesion forces we are dealing with are mostly VDW forces. In addition, we find no evidence for a significant number of covalent bonds removed during the contact mode AFM experiments.

The first column in Table 3 shows that all four types of silane surface treatments improve the adhesion of PP to the substrate relative to its adhesion to bare glass although not by the same degree. While the improvement achieved using the hydrophilic treatments (APS, GPS) is only minor, considerable increases in adhesion strengths are observed for the two alkyl silane treatments (VS, TPS). From these results it is obvious that the hydrophobic PP favors the more hydrophobic silane treatments, and the strength of interaction between the PP and the alkyl groups is stronger than its interaction with polar groups. These results are supported by the surface characteristics (roughness RMS and P-V) presented in Table 2 and discussed above.

As the adhesion strength results indicate, there is no benefit in using functionalized silane (amino or epoxy groups in APS and GPS) since PP remains inert at temperatures in excess of 200°C [20], which are commonly employed in PP processing. Moreover, commercial PP used in the composite industry usually contains additives such as antioxidants, which suppress possible radical reactions through the relatively weak tertiary carbon in PP [21].

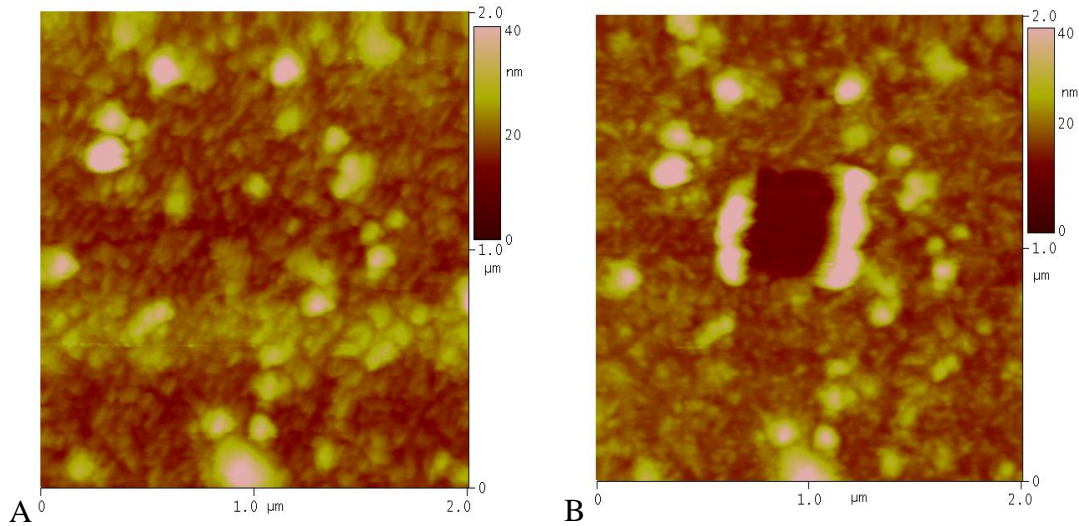


Fig.2. Adhesion strength evaluation: AFM images of PE on untreated glass: A) before, B) after the contact-mode AFM scan.

Turning our attention to PP-g-ma we find that the attraction of the grafted polar functional groups to the more hydrophilic silane treatments is sufficient to overcome the natural tendency of the PP backbone despite the relatively small fraction of grafting.

The adhesion strength of PP-g-ma to the two alkyl silane treatments (VS, TPS) is smaller than that of PP. On the other hand, its adhesion strength to the hydrophilic surfaces is more than twofold larger than that of PP. The values measured for the hydroxyl (untreated glass), amino (APS), and epoxide (GPS) functional groups can be attributed to the hydrogen bonding between these groups and the maleic anhydride graft. The interaction of PP-g-ma with the surface is the sum of two opposing contributions: the interaction of the PP backbone, which increases with increasing hydrophobicity from glass to TPS, and that of maleic anhydride in the opposite direction. As a result of these two opposing trends, optimal adhesion for PP-g-ma is obtained using the mildly hydrophilic GPS (52^o water wetting).

For every substrate examined in this research, the adhesion force of LDPE is several times larger than the corresponding force for PP. With the exception of GPS, the hydrophobic LDPE exhibits a tendency toward the more hydrophobic silane treatments. The strength of adhesion of a polymer molecule is a function of the number of anchoring sites per molecule and the strength of each individual contact. Since the chemical natures of PP and PE units are not very different, we assume that the strengths of individual contacts are of the same order of magnitude for both. Thus, we assume that the higher adhesion strength is due to higher numbers of contacts between the surface and the polymer chain and its branches. Yet, as pointed out above (cf. discussion of Table 1), it is difficult to estimate the number of contacts for LDPE due to the lack of information on the extent of branching, and we have no means to verify that the greater contact numbers are indeed responsible for the large increase in adhesion strength relative to PP. Note that while PP is completely inert at temperatures ca. 200^oC, branched PE molecules such as LDPE tend to crosslink at these temperatures [22], especially in the presence of highly reactive end groups such as epoxides (GPS). This may offer an alternative explanation of the results for LDPE in contact with the more reactive surfaces.

PE-g-ma consistently showed the lowest adhesion strength measured here irrespective of the type of surface treatment. The measured value of 7nN force is only slightly above the experimental detection limit and only moderately above the thermal energy of boiling o-xylene, the solvent for this polymer. We conclude that the short PE-g-ma chains are surface anchored only in a small number of sites. This quantity is sufficient to overcome the kT barrier but not large enough to affect the adhesion strength due to specific interactions of the maleic anhydride with surface functional groups.

Table 3: Force (in nN) applied by the AFM to remove the polymer from a glass surface ($\pm 3nN$).

Surface Treatment	PP	PP-g-ma	LDPE	PE-g-ma	PS
Untreated glass	14	39	66	7	7
APS	17	40	73	7	39
GPS	17	52	134	7	15
VS	38	32	104	7	22
TPS	38	25	97	7	7

With the exception of APS, the adhesion of PS is consistently weaker than that of PP and does not correlate with the polarity of the silane treatment. Since the number of contacts per chain is similar in both cases (Table 1), the difference probably lies in the strength of individual contacts or, in other words, in the nature of the specific interactions between the aromatic rings on the polymer and the functional groups on the surface. These interactions include hydrogen bonding between the surface groups and the π system of benzene, strong VDW interactions induced by conjugated π bonds, and phenyl stacking effects.

CONCLUSIONS

Bare glass slides were treated with organofunctional silanes by sililation from aqueous solutions. The silane film covalently bonded onto the glass appears to be composed of polysiloxane network domains connected laterally on the surface. Static contact angle measurements, XPS, force-distance measurements, and topographic AFM imaging have confirmed the formation of a silane layer coating the glass surface. Overall, the silane sizing conforms to the glass surface topology. The systematic increase in water contact angle relative to the different treated surfaces is well correlated with the type of organic functional end group of the different silane treatments.

Each of the three homopolymers tested here was found to have a characteristic layer thickness irrespective of the type of the surface treatment onto which it was deposited. We claim that polymer layer thickness is a result of the procedure used for polymer deposition, which left only highly adsorbed chains with large numbers of anchoring points on the surface. As a result, numerous VDW interactions are formed between the polymer and the surface, the strength of which depend on the specific interactions. The strength of these interactions was revealed by contact-mode AFM adhesion strength experiments. Hydrophobic PP and LDPE showed affinity towards the more hydrophobic silane surfaces, whereas the relatively small number of polar maleic anhydride molecules included in PP-g-ma increased its affinity toward hydrophilic treatments. Significant increase in adhesion strength was observed in PP-g-ma and LDPE in comparison to PP. PS interactions with the surface were dominated by the conjugated π system-induced proton donor-acceptor relationship. The contact-mode AFM technique used here was shown to provide useful information on molecular level polymer-surface interactions.

ACKNOWLEDGEMENTS

This research was supported by the Israel Science Foundation (grant No. 193/01). This work has also been partially funded by the Reimund Stadler Minerva Center for Mesoscale Macromolecular Engineering. Minerva is funded through the BMBF. We thank Y. Yagen, M. Yudovich for help in samples preparation and J. Jopp for his advice and help in carrying out AFM and OPIM measurements.

REFERENCES

1. Berger ES, Petty EH. In: Katz HS, Milewski JV, editors. *Handbook of fillers for plastics*, New York: Van Nostrand Reinhold Company, 1987.
2. Miller AC, Berg JC. *Composites* 2003; 34A: 327-332.
3. Fuad MYA, Ismail Z, Ishak ZAM, Omar AKM. *Eur. Polym. J.* 1995; 31: 885-893.
4. Mader E, Jacobasch HJ, Grudke K, Gietzelt T. *Composites* 1996; 27A: 907-912.
5. Demjen Z, Pukanszky B, Nagy J. *Composites* 1998; 29A: 323-329.
6. Hornsby PR, Hinrichsen E, Tarverdi K. *J. Mater. Sci.* 1997; 32: 1009-1015.
7. Cantero G, Arbelaiz A, Llano-Ponte R, Mondragon I. *Compos. Sci. Technol.* 2003; 63: 1247-1254.
8. Pisanova E, Zhandarov S, Mader E, Ahmad I, Young R. *J. Composites* 2001; 32A: 435-443.
9. Dvir H, Jopp J, Gottlieb M. *J. Colloid Interface Sci.* 2006; 304:58-66.
10. Fetters LJ, Lohse DJ, Colby RH. Chain dimensions and entanglement spacings. In: Mark JE, editor. *Physical properties of polymers handbook*, 2nd ed. Springer: 2007. pp. 447; also: http://felix.metsce.psu.edu/rheology/principal/papers_local/MeReview.pdf
11. <http://www.optotl.ru/MatEng.htm>
12. De Gennes PG. *Scaling concepts in polymer physics*, Ithaca and London: Cornell University Press, 1979.
13. Fler GJ, Cohen Stuart MA, Scheutjens JMHM, Cosgrove T, Vincent B. *Polymers at interfaces*, London: Chapman & Hall, 1993.
14. Aubouy M, Guiselin O, Raphael E. *Macromolecules* 1996; 29: 7261-7268.
15. Jones R. *Curr. Opin. Colloid Interface Sci.* 1999; 4: 153-158.
16. De Gennes PG. *Macromolecules* 1981; 14: 1637-1644.
17. Guiselin O. *Europhys. Lett.* 1992; 17: 225-230.
18. Alexander S. *J. Phys. (Paris)*. 1977; 38: 983-987.
19. Anariba F, Duval SH, McCreery RL. *Anal. Chem.* 2003; 75: 3837-3844.
20. Cartier H, Hu GH. *Polym. Eng. Sci.* 1998; 38: 177-185.
21. Dvir H, Gottlieb M, Daren S. *J. App. Polym. Sci.* 2003; 88: 1506-1515.
22. Abad MJ, Ares A, Barral L, Cano J, Diez FJ, Garcia-Garabal S, Lopez J, Ramirez C. *J. App. Polym. Sci.* 2004; 92: 3910-3916.